Available online at www.sciencedirect.com
ScienceDirect
Journal of Nuclear Materials 362 (2007) 416–425
journal of nuclear materials
www.elsevier.com/locate/jnucmat

Thermal diffusion of chlorine in uranium dioxide studied by secondary ion mass spectrometry and X-ray absorption spectroscopy

Y. Pipon [a,*], N. Toulhoat [a,f], N. Moncoffre [a], L. Raimbault [b], A.M. Scheidegger [c], F. Farges [d], G. Carlot [e]

[a] Institut de Physique Nucléaire de Lyon (IPNL), 4, rue Enrico Fermi, 69622 Villeurbanne cedex, France
[b] Centre d'Informatique Géologique (CIG), Ecole des Mines, 35 rue Saint Honoré, F-77305 Fontainebleau cedex, France
[c] Laboratory for Waste Management, Nuclear Energy and Safety Department (NES), Paul Scherrer Institut CH-5232 Villigen PSI, Switzerland
[d] Laboratoire des Géomatériaux, Université de Marne la Vallée, 5 Bd Descartes-Champs S/Marne, 77454 Marne la Vallée cedex 2, France
[e] Commissariat l'Energie Atomique (CEA), Centre de Cadarache, DEN/DEC/SESC/LLCC, 13108 Saint-Paul lez Durance, France
[f] Commissariat l'Energie Atomique (CEA), DEN/Saclay, 91191 Gif s/Yvette Cedex, France

Abstract

In a nuclear reactor, ^{35}Cl present as an impurity in the nuclear fuel is activated by thermal neutron capture. During interim storage or geological disposal of the nuclear fuel, ^{36}Cl may be released from the fuel to the geo/biosphere and contribute significantly to the 'instant release fraction'. In order to elucidate the diffusion mechanisms, both irradiation and thermal effects must be assessed. This paper deals with the thermal diffusion of chlorine in depleted UO_2. For this purpose, sintered UO_2 pellets were implanted with ^{37}Cl at an ion fluence of 10^{13} cm^{-2} and successively annealed in the 1175–1475 K temperature range. The implanted chlorine is used to simulate the behaviour of the displaced one due to recoil and to interactions with the fission fragments during reactor operation. The behaviour of the pristine and the implanted chlorine was investigated during thermal annealing. SIMS and μ-XAS (at the Cl–K edge) analyses show that:

(1) the thermal migration of implanted chlorine becomes significant at 1275 K; this temperature and the calculated activation energy of 4.3 eV points out the great ability of chlorine to migrate in UO_2 at relatively low temperatures,
(2) the behaviour of the implanted chlorine which aggregates into 'hot spots' during annealing before its effusion is clearly different from that of the pristine one which remains homogenously distributed after annealing,
(3) the 'hot spot' and the pristine chlorine seem to be in different structural environments. Both types of chlorine are assumed to have a valence state of −I,
(4) the comparison between an $U_2O_2Cl_5$ reference compound and the pristine chlorine environment shows a contribution of the $U_2O_2Cl_5$ to the pristine chlorine.

* Corresponding author. Tel.: +33 4 72431057; fax: +33 4 72448004.
E-mail address: pipon@ipnl.in2p3.fr (Y. Pipon).

0022-3115/$ - see front matter © 2007 Elsevier B.V. All rights reserved.
doi:10.1016/j.jnucmat.2007.01.212

PACS: 61.10.Ht; 81.05.Je; 66.30.−h; 82.80.Ms

1. Introduction

Among fission or activation products such as ^{129}I, ^{135}Cs, ^{99}Tc, ^{14}C and ^{36}Cl, ^{129}I and ^{36}Cl dominate annual dose rates at the outlet in most reference and degraded scenarii of spent fuel disposal [1]. Due to its solubility and poor retention in the near field, ^{36}Cl is known to contribute significantly to the instant release fraction. Moreover, due to its volatile behaviour, it is likely to be released to the atmosphere in case of a reactor incident. It is therefore important to assess its behaviour during in pile processes.

Pristine chlorine (^{35}Cl: 75.77% and ^{37}Cl: 24.23%) is present as an impurity in the nuclear fuel (<5 ppm). During reactor operation, ^{36}Cl is produced by neutron capture according to the $^{35}Cl(n, \gamma)^{36}Cl$ reaction which has a rather large cross-section for thermal neutrons (around 33 barns). During in pile processes, part of the ^{36}Cl atoms will be displaced from their original positions due to recoil or to collisions with the fission products. The chlorine atoms are therefore likely to occupy different sites in the fuel structure and may have different chemical states. In this study, implanted ^{37}Cl was used to simulate the behaviour of the displaced chlorine. The main results obtained by secondary ion mass spectrometry (SIMS) on the thermal behaviour of chlorine are presented together with information on the structural environment obtained by micro X-Ray absorption spectroscopy (XAS).

In a previous paper [2], the great ability of the implanted chlorine to diffuse was pointed out in comparison with fission products as iodine or xenon. Chlorine becomes mobile from temperatures as low as 1275 K. SIMS results showed the contrasted behaviour between the implanted ^{37}Cl and the pristine one simulated by ^{35}Cl. ^{37}Cl diffuses to the grain boundaries and aggregates near the surface of the samples after annealing in the temperature range 1275–1475 K before its release at higher temperatures. In this paper, complementary information is given on the chemical state and the environment of the pristine and implanted chlorine obtained by μ-XAS.

2. Experimental procedures

In order to simulate the thermal diffusion of chlorine in UO_2, sintered depleted (0.3% ^{235}U) UO_2 pellets of 8 mm diameter and 1 mm thickness were used. The samples have been polished and successively annealed at a temperature of 1775 K under H_2 atmosphere in order to anneal the defects resulting from polishing.

In order to control the surface stoichiometry of the samples, XPS measurements have been performed on the pellets before and after implantation and annealing. The results (not shown here) indicate a slight deviation from stoichiometry for the uranium dioxide which is under the form of UO_{2+x}. It is to note that the initial stoichiometry of the virgin pellets remains unchanged after implantation and annealing.

The samples were implanted with $^{37}Cl^+$ at the Nuclear Physics Institute of Lyon (implantation energy of 270 keV) with an ion fluence of 10^{13} cm^{-2} for SIMS analyses and 10^{14} cm^{-2} to improve the signal to noise ratio for XAS experiments. The ^{37}Cl projected range (R_p) calculated with SRIM [3] is 150 nm and the maxima of the ^{37}Cl concentration in atomic percent is 0.0007 (7 ppm). The implantation ion fluence of 10^{13} cm^{-2} was chosen in order to minimize probable effects due to release and/or trapping usually observed at high ion fluences (above 10^{14} cm^{-2}) for volatile fission products (as Xe and I).

The implanted samples were then annealed in a tubular furnace in the 1175–1475 K temperature range under secondary vacuum (around 10^{-10} bar) degraded by a H_2 flow (until around 10^{-9} bar). These conditions allow maintaining the stoichiometry of UO_2 [4].

Dynamic SIMS was carried out to study the spatial distribution of ^{37}Cl in untreated 'virgin' samples, in as-implanted and in annealed samples.

Moreover and, in order to obtain molecular-level information on the speciation and the structural environment of chlorine in UO_2, μ-XRF and μ-XAS experiments at the chlorine K-edge (2.822 keV) were performed at the LUCIA beamline at the swiss light source (SLS), Paul Scherrer Institut (PSI), Villigen, Switzerland. The beamline has

been designed to deliver a photon flux of the order of 10^{12} s^{-1} on a few μm^2 spot size within the energy domain of 0.8–8 keV [5]. The μ-XRF/XAS experiments were performed using the Si(1 1 1) crystal pair in a water cooled fixed-exit double-crystal monochromator.

The final focusing of the X-ray beam was done using a Kirkpatrick–Baez (KB) system. In the study, beam size used for the μ-XRF/XAS investigations was $\sim 5 \times 7$ μm^2.

XAS data were analyzed using the ATHENA software [6] and XAFS 3.0 software [7]. Two to ten spectra were averaged before being background subtracted and then normalized using standard procedures. The inflection point of the Cl–K absorption edge for each spectrum was determined from the energy of the maximum of the first derivative.

To understand geometric and electronic structure effects, XAS simulations were performed using the FEFF 8.2 code [8]. This includes the use of self-consistent muffin-tin potentials, full multiple scattering theory and $Z + 1$ approximation.

Continuous Cauchy wavelet transforms (CCWT) was also computed on the normalized XAS spectra. As compared to conventional Fourier transform (FT) procedures, WT provides a more detailed analysis of the XAS signals, with a reciprocal space-direct space 3D correlation [9]. Among others, this procedure allows to discriminate the backscattering neighbouring atoms (here: U, O, etc.) around the central absorbing atom (here: Cl).

3. Results

3.1. SIMS results

In a previous paper, the great ability of the implanted chlorine to migrate was pointed out [2]. Mobile anion vacancies have been suggested to provide preferential paths for anion directed migration. After a 10 h annealing at 1475 K, most of the chlorine has disappeared from the sample. At that point, the measured ratio of the implanted chlorine (^{37}Cl) versus the original one (^{35}Cl) is 1.2 whereas the natural isotopic ratio is 0.3. This shows that a certain amount of the implanted ^{37}Cl remains in the sample. A comparison of the maps corresponding to the ionic distributions of $^{37}Cl^-$, $^{35}Cl^-$ and $^{254}(UO)^-$ before and after 10 h annealing at 1475 K is presented in Fig. 1. It can be seen that the pristine ^{35}Cl and the implanted ^{37}Cl are homogeneously distributed in the grains before annealing (Fig. 1(a) and (c)). After annealing, ^{35}Cl is still homogeneously distributed (Fig. 1(f)) whereas ^{37}Cl aggregates into 'hot spots' (Fig. 1(d)). Moreover, these

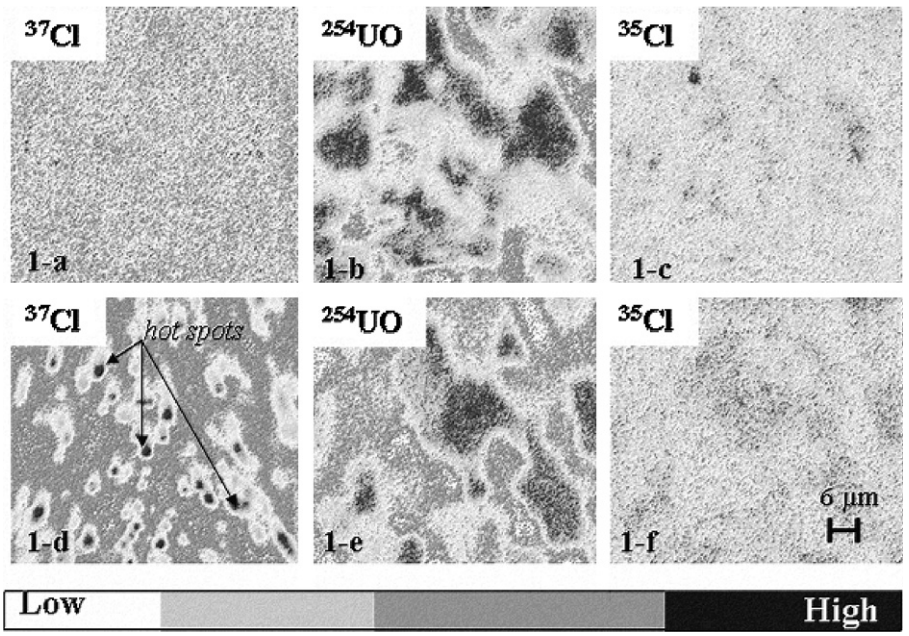

Fig. 1. Concentration maps of ^{37}Cl, ^{254}UO and ^{35}Cl made by SIMS on an as-implanted UO_2 sample (top pictures (a–c)) and on an annealed UO_2 sample (bottom pictures (d–f)). A relative concentration scale is indicated with dark grey standing for a high concentration.

aggregates do not seem to be gaseous, as no 'flash' of chlorine was observed during analysis.

This behaviour points out the necessity to identify the structural environment and the chemical state of the pristine, the implanted and the chlorine in the 'hot spots'.

3.2. μ-XRF mappings and μ-XAS spectra

μ-XAS experiments were performed on one hand on 'virgin' and, on the other hand, on implanted and annealed UO_2 samples as well as on following reference compounds:

- NaCl and $NaClO_4$, because of their different valences, namely Cl(−I), Cl(+VII),
- $LaCl_3$, which is isostructural to UCl_3 (Cl(−I)),
- UCl_4 and $U_2O_2Cl_5$; these two last compounds were carefully handled under an He or N atmosphere because of their hygroscopicity. Uranium occurs in two valences, +IV and +V, in $U_2O_2Cl_5$ [10]. This last type of compounds as well as other uranium oxichlorides (such as UOCl, UO_2Cl, $UOCl_3$, UO_2Cl_2, etc.) and chlorides (such as UCl_5) or a mixture of them might be formed during annealing. However, UO_2Cl is not stable at temperatures higher than 923 K and UO_2Cl_2 decomposes at temperatures higher than 773 K [10].

The structural information and the environment of chlorine in these samples are presented on Table 1 (information on uranium references are taken from the thesis of Levet [10]). The measured energies of the absorption edges (see the experimental procedure) are shown on Table 2. Different experimental sessions result in a reproducibility in edge position of about 0.3 eV.

Fig. 2(a) presents the Cl K-edge XAS spectra collected on $U_2O_2Cl_5$, UCl_4 and $LaCl_3$. The shape of the XAS spectra of $U_2O_2Cl_5$ and UCl_4 are quite similar and they have the same absorption edge position. On these compounds spectra, a more or less pronounced shoulder is also present on the absorption edge. This could reflect transitions to molecular orbitals with both Cl 3p and metal character as suggested by Shadle et al. [11]. This author has shown that pre-peak feature (not observed here), well separated from the rising edge, is absent in metal systems with a full d-manifold. To confirm that, the $LaCl_3$ spectrum does not display any pre-peak or shoulder because the La^{3+} electronic configuration is that of the rare gas Xe which does not have an open shell. The ground state electronic structure of uranium is the following: $[Rn]\cdot 5f^3\cdot 6d^1\cdot 7s^2$. In UO_2 and in the uranium reference compounds, the formal charge carried by uranium ions is between +4 and +5. This means that the configuration is between $[Rn]\cdot 5f^0$ and $[Rn]\cdot 5f^2$ reflecting a semi-conductor behaviour and an open f shell. The shoulder displayed on the XAS spectra of the U reference compounds could be assigned to transitions to molecular orbitals reflecting bonds between Cl and U.

Table 1
Structural information of the reference compounds used for the μ-XAS experiments (valence, crystallographic system and chlorine environment in the lattice)

Compounds	Cl valence	Crystallographic system (space group)	Chlorine environment	Distances (Å)
$LaCl_3$	−I	Hexagonal (P63/m)	Cl bond to 2 Cl atoms	R(Cl–Cl) = 2.19
UCl_4	−I	Tetragonal (I4/amd)	Cl bond to 2 U atoms	R(Cl–U) = 2.64
$U_2O_2Cl_5$	−I	Orthorhombic (Cmmm)	2 different sites where Cl is bond to U atoms	R_1(Cl–U) = 2.68 R_2(Cl–U) = 2.73
NaCl	−I	Cubic ($Fm\bar{3}m$)	Cl surrounded by 6 Na atoms	R(Cl–Na) = 2.82
$NaClO_4$	+VII	Orthorhombic (Cmcm)	Cl bond to 2 O atoms and to 2 others O atoms	R_1(Cl–O) = 1.43 R_2(Cl–O) = 1.44

Table 2
Energy positions of the absorption edges of the experimental reference compounds and the UO_2 samples

Compound	$LaCl_3$	Cl–UO_2 virgin	Cl–UO_2 annealed	NaCl	UCl_4	$U_2O_2Cl_5$	$NaClO_4$
E_0 (eV)	2822.5	2822.5	2823.5	2824.5	2824.5	2824.5	2833.0

Different experimental sessions result in reproducibility in edge position of about 0.3 eV.

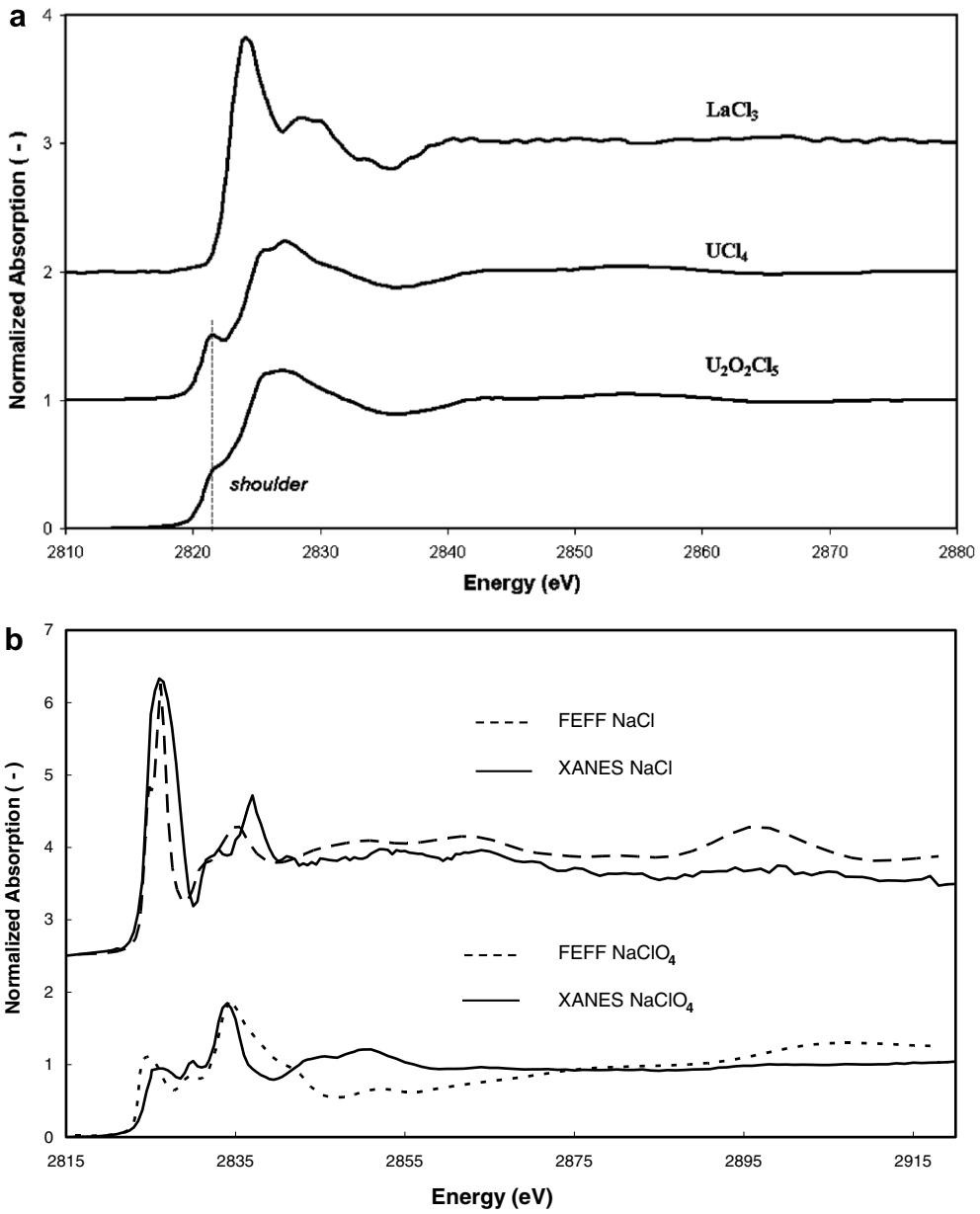

Fig. 2. XAS spectra of several references compounds and some of their associated FEFF simulations. (a) Spectra of $LaCl_3$, UCl_4 and $U_2O_2Cl_5$. (b) The comparison of the XAS spectra and FEFF simulation on NaCl and $NaClO_4$.

Fig. 2(b) shows the NaCl and $NaClO_4$ XAS spectra and their respective FEFF simulations. NaCl and $NaClO_4$ are well-known common reference compounds for chlorine usually used to calibrate FEFF simulations of chlorine XAS spectra. First of all, FEFF simulation of NaCl was performed with an 81 atoms lattice. The NaCl FEFF spectrum is quite coherent with the experimental spectrum except for the main peak after the edge which is broader on the experimental spectrum. The $NaClO_4$ FEFF simulation does not fit perfectly the experimental spectrum but is nevertheless quite coherent with it. This difference between the two spectra is due to the fact that it was not possible to analyze a pure end member as this compound contained some impurities among them NaCl.

The comparison between the experimental NaCl and $NaClO_4$ spectra shows that the edge energy is

shifted from 2822.3 eV on $LaCl_3$ and 2824.5 eV on NaCl to 2833 eV on $NaClO_4$ reflecting the shift of the formal charge of chlorine which is −I in NaCl and $LaCl_3$ to +VII in $NaClO_4$. This type of shift has been used in the literature to evaluate a dependence between the absorption edge energy and the charge of the element. Some studies on other elements such as molybdenum, manganese and plutonium [12–14] have pointed out a linear dependence between the X-ray edge position and the quantity called the 'coordination charge'. This effect was already observed by Shadle et al. [11] who noted a 10 eV shift in the absorption edge energies of KCl and $NaClO_4$. Myneni [15] also reports respective edge energies of 2822.3 eV and 2832 eV for Cl in −I (KCl) and +VII ($NaClO_4$). Nefedov et al. [16] measured 'more realistic' charges on Cl compounds using Auger spectroscopy. The charge on Cl in KCl, $KClO_3$ and $KClO_4$ was determined to be −0.87, +1.49 and +1.91, respectively. Shadle et al. determined a linear relationship between these realistic Cl charges and the corresponding measured absorption edge energies [11]. According to the equation determined by Shadle et al. ($q = -916.66 + 0.32425\ eV^{-1}(x)$ where q is the charge on Cl and x the edge position in eV), the difference between the absorption edges of Cl(0) and Cl(−I) is around −3 eV. Chlorine in a formal charge of +I should have an edge position around 2830 eV. However, other works of Huggins et al. [17] and Filipponi et al. [18] show that the relationship between absorption edge and charge seems not to be linear anymore for low valences of chlorine. These authors, investigated references such as $Ca(ClO)_2$ with Cl(+I), $NaClO_2$ with Cl(+III) and $NaClO_3$ with Cl(+V). Table 3 resumes the absorption edge energies of chlorine references from the literature and from this work for Cl charges in the range (−I)–(+VII). This table shows that the absorption edge energy of NaCl is higher than that of $Ca(ClO)_2$ and that the linear relationship determined by Shadle et al. cannot be used for Cl valences between (−I) and (+I).

μ-XRF maps ($600 \times 600\ \mu m^2$) at 3 keV collected on the 'virgin' and the as-implanted samples confirmed the expected homogeneous chlorine distribution. Consequently, for both 'virgin' and as-implanted samples, μ-XAS spectra were collected on random areas of the samples.

As the pristine chlorine is present as impurity at the ppm level in UO_2, several spectra were collected on the same spot of the 'virgin' UO_2 to check for potential kinetic effects of the beam (Fig. 3). An evolution of the spectrum under the beam can be observed during the analysis. The edge crest of the first scan is composed of a singlet, centered at 2827 eV. It decomposes with time after about one hour (cf Fig. 3 – 3rd scan) into a doublet (2824.5 and 2827 eV). The last scan shows a less intense XAS feature at 2827 eV and a shoulder at its higher energy (2832 eV) side appears. Because of this relatively slow evolution, for further interpretation, only the first scan will be considered as representative of the pristine chlorine.

The XAS spectra for the as-implanted sample are similar to those for the 'virgin'. This is because the depth probed by Cl–K edge XAS in fluorescence mode (a few micrometers) is much greater than the actual implanted depth (400 nm). Therefore, the main contribution to the XAS signal comes from the pristine chlorine.

An XRF map collected on the sample that was both implanted and annealed shows that chlorine is heterogeneously distributed with a number of 'hot spots' (presented in a previous paper [2]). The size of the chlorine-enriched hot spots strongly varies from a few nm in diameter up to sizes over 100 nm. Based on more spatially resolved SIMS maps, these 'hot spots' correspond to aggregates of smaller Cl-enriched 'clusters'.

For the annealed sample, different chlorine enriched 'hot spots' were selected for μ-XAS investigations.

μ-XAS spectra were performed on a selected 'hot spot' of the annealed sample. As it has been observed for the virgin sample, an evolution of the spectrum under the beam can be observed as shown on Fig. 4. A doublet with one peak centred at 2824 eV and a more intense one centred at 2826 eV decomposes after about one hour into a

Table 3
Energy positions of the absorption edges with their associated errors of some chlorine references

Compound	NaCl	Cl_2 (gaseous)	$Ca(ClO)_2$	$NaClO_2$	$NaClO_3$	$NaClO_4$
Chlorine valence	−I	0	+I	+III	+V	+VII
Reference	This work	[17]	[17]	[18]	[18]	This work
E_0 (eV)	2824.5 ± 0.3	2820.7 ± 0.2	2821.9 ± 0.2	2825.9 ± 0.2	2830.2 ± 0.2	2833.0 ± 0.3

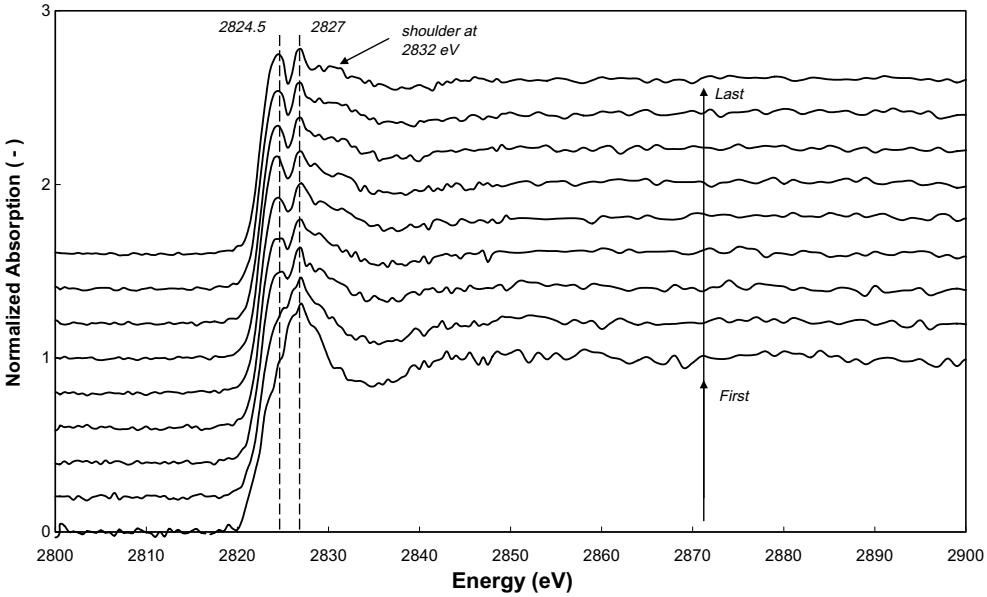

Fig. 3. XAS spectra showing the evolution of the pristine chlorine under the photon beam.

doublet where the first peak of the doublet, which is centred at 2825 eV, is very intense whereas the second one centred at 2828 eV is less intense. Moreover, a pre-edge feature labelled A appears. As previously, the first scan will be considered as representative of the 'hot spot' chlorine.

The 'hot spot' first scan XAS spectrum of the annealed sample is compared to the pristine chlorine XAS spectrum of the virgin sample on Fig. 4. The shape of the spectrum of the annealed UO_2 is quite different from the 'virgin' one with an E_0 energy shift of +1 eV of the annealed sample with respect to the virgin UO_2 (Table 1).

Therefore, it can be assumed that the chlorine in the 'hot spots' and in the virgin UO_2 have two different environmental configurations.

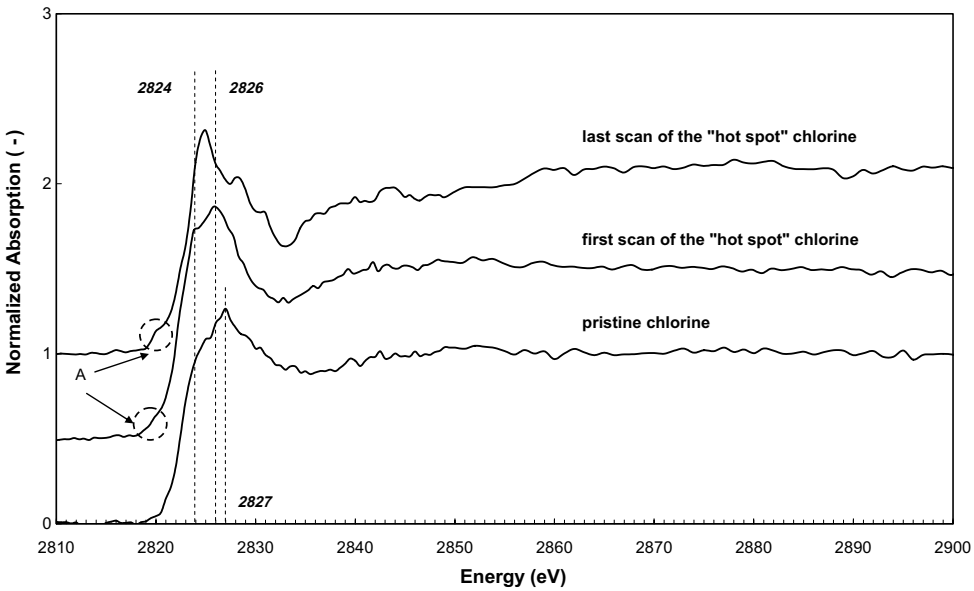

Fig. 4. Comparison of the XAS spectra of the pristine chlorine in the 'virgin' UO_2, the first scan and the last scan of the 'hot spot' chlorine in the implanted and annealed UO_2.

3.3. Wavelet transforms

Wavelets (WT) have been used in order to investigate the first neighbours and their respective distance to chlorine. WT have been computed on the 'virgin' and on the implanted-annealed UO_2 as well as on NaCl, UCl_4 and $U_2O_2Cl_5$ to help with the identification of the next-nearest neighbours. Despite of its limited *k*-range, WT of the XAS provide insights on the local structures, particularly in highly locally disordered system such as chlorine in UO_2 [9].

Fig. 5(a) shows the 2D WT picture of the NaCl FEFF data used as a reference. NaCl is the perfect compound for that because the two main contributions of the XAS spectrum come from simple scattering pairs which are Na–Cl (theoretical distance = 2.82 Å) and Cl–Cl (theoretical distance = 3.89 Å). The two intense contributions (around 2.5 Å and 3.5 Å) correspond to the backscattering pairs (Na–Cl) and (Cl–Cl). The comparison of these distances with the formal ones (Table 4) allows to deduce the phase-shift around 0.35 Å. The less intense contribution (around 1.5 Å) is probably an artefact.

Similar analyses have been made for UCl_4 and $U_2O_2Cl_5$. Fig. 5(b) and (c) shows the WT of the two compounds. For $U_2O_2Cl_5$ (Fig. 5(b)), the backscattering pair around 2.3 Å (2.65 when corrected by phase-shift) corresponds to the Cl–U bond (2.68–2.73 Å). For UCl_4 (Fig. 5(c)), the backscattering pair around 2.2 Å (2.55 when corrected by phase-shift) corresponds to the Cl–U bond (2.64 Å).

The WT performed on the 'virgin' sample for the first scan is presented in Fig. 5(d). A single backscattering contribution can be observed around 2.3 Å, which could correspond to uranium first neighbours.

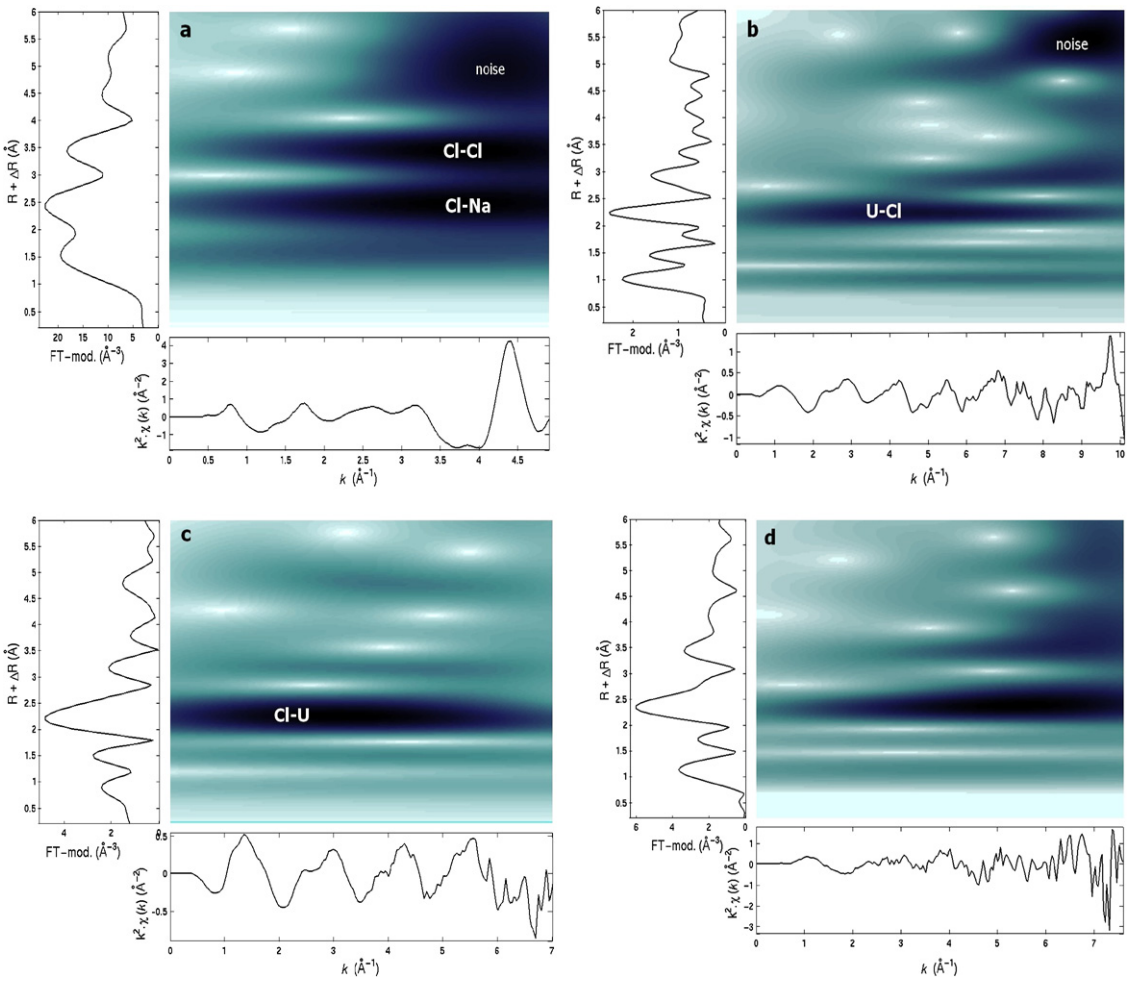

Fig. 5. Wavelet transforms performed on references and on the 'virgin' UO_2. (a) FEFF NaCl spectrum, (b) $U_2O_2Cl_5$, (c) UCl_4, (d) first scan of the pristine chlorine in the 'virgin' UO_2.

Table 4
Chlorine-first neighbours bond lengths in the references

Shell	First next neighbour distances (Å)	Second next neighbour distances (Å)	Third next neighbour distances (Å)
NaCl	R(Cl–Na) = 2.82	R(Cl–Cl) = 3.89	
$NaClO_4$	R_1(Cl–O) = 1.43		
	R_2(Cl–O) = 1.44		
$U_2O_2Cl_5$	R_1(Cl–U) = 2.68	R(Cl–Cl) = 3.21	R(Cl–O) = 3.43
	R_2(Cl–U) = 2.73		
UCl_4	R(Cl–U) = 2.64	R(Cl–Cl) = 3.10	

The WT performed on the first scan of a 'hot spot' is not shown due to the very noisy background.

4. Discussion and conclusion

Based on the presented SIMS, XAS and WT data, the following has been observed:

- The position of the edge energy reflects a negative charge for the chlorine in all reference compounds except for $NaClO_4$. Using the linear relationship of Shadle et al., pristine chlorine and chlorine present in the 'hot spots' would display a negative charge, This agrees also with the edges of $LaCl_3$, UCl_4 and $U_2O_2Cl_5$ where Cl has a negative charge. However, according to the data obtained by Huggins and Huffman [17] and Filipponi et al. [18], the linear relationship between valence and edge energy is not straitforward for low Cl valences. The assumed negative charge of the pristine and 'hot spot' chlorine has therefore to be confirmed by analysing other references with low Cl valences.
- XAS spectra of pristine and hot spot chlorine probably exhibit two distinct entities of Cl species. Each type of chlorine seems to be in an ordered structural environment.
- Comparing the pristine and hot spot spectra to the $LaCl_3$ spectrum, it can been deduced that there are no species such as UCl_3 (as $LaCl_3$ is isostructural to UCl_3).
- The differences regarding edge position and edge shape probably reflect a change in coordination state between the two species present in the 'virgin' and in the implanted-annealed UO_2 samples.
- A clear influence of the photon beam has been evidenced on the pristine chlorine: the progressive decomposition of a singlet into a doublet. The WT performed on the first scan seems to indicate a distance around 2.3 Å (not corrected for phase-shift) which could be a Cl–U bond. A hypothesis can be made to explain the evolution of the spectrum under the beam: E. M. Moujahid et al. [19] have shown a similar spectrum (with a doublet and a shift of −2 eV of the energy of the absorption edge with respect to NaCl) for $ZnCl_2$. This evolution was interpreted by a 'dynamic behaviour' of the interlayer Cl-anions (shown by NMR spectroscopy by Kirkpatrick et al. [20]) initiated by a thermal treatment which could, in the present study, correspond to the X-Ray photo-evolution.
- The influence of the beam has also been evidenced in the case of chlorine in the hot spots with a clear change in the shape of the spectrum.

Following main conclusions may be inferred from the data:

(1) The wavelet transforms (WT) of $U_2O_2Cl_5$ and pristine chlorine display similarities. This could indicate that the chlorine environment of the pristine chlorine is close to $U_2O_2Cl_5$.
(2) Both pristine and 'hot spot' chlorine display most probably a negative valence. This fact agrees with the hypothesis of anionic transport of chlorine along mobile anion vacancies induced by the implantation defects.
(3) A drawback of these experiments is a poor or noisy EXAFS signal. The use of a cryostat would allow to minimize or to avoid the evolution of the spectra during beam irradiation. It would may be allow to get a better EXAFS signal on the chlorine in the hot spots.

Acknowledgements

The authors are very grateful to Henri Noël (Laboratoire de Chimie du Solide et Inorganique Moléculaire (LCSIM), University of Rennes) for

providing the uranium reference compounds. We also thank A.M Flank, P. Lagarde for their great help during the experiments at the LUCIA beamline, PSI.

References

[1] L. Johnson, C. Poinssot, C. Ferry, P. Lovera: Estimates of the instant release fraction for UO_2 and MOX fuel at $T = 0$, A Report of the Spent Fuel Stability [SFS] Project of the 5th Euratom Framework Program, Nagra Technical Report NTB 04–08, March 2005, Wettingen.
[2] Y. Pipon, N. Toulhoat, N. Moncoffre, H. Jaffrézic, S. Gavarini, P. Martin, L. Raimbault, A.M. Scheidegger, Radiochim. Acta 94 (2006) 705.
[3] J.F. Ziegler, J.P. Biersaack, U. Littmark, 'The Stopping and Range of Ions in Solids', New York, 1985.
[4] C. Poinssot, P. Toulhoat, J.P. Grouiller, J. Pavageau, J.P. Piron, M. Pelletier, P. Dehaudt, C. Cappelaere, R. Limon, L. Desgranges, C. Jegou, C. Corbel, S. Maillard, M.H. Faure, J.C. Ciccariello, M. Masson, PRECCI Report CEA-R-5958 (E) 1, 2001, 168.
[5] A.-M. Flank, G. Cauchon, P. Lagarde, S. Bac, M. Janousch, R. Wetter, J.-M. Dubuisson, M. Idir, F. Langlois, T. Moreno, D. Vantelon, Nucl. Instrum. and Meth. B 246 (2006) 269.
[6] B. Ravel, M. Newville, J. Synchrotron Radiat. 12 (2005), Part 4.
[7] M. Winterer, J. Phys. IV France 7 (1997), C2.
[8] A.L. Andukinov, B. Ravel, J.J. Rehr, S.D. Conradson, Phys. Rev. B 58 (1998) 7656.
[9] M. Munoz, P. Argoul, F. Farges, Am. Mineral. 88 (2003) 694.
[10] J.C. Levet, PhD Thesis, University of Rennes (1978).
[11] S.E. Shadle, B. Hedman, K.O. Hodgson, E.I. Solomon, Inorg. Chem. 33 (1994) 4235.
[12] S.P. Cramer, T.K. Eccles, F.W. Kutzler, K.O. Hodgson, L.E. Mortenson, J. Am. Chem. Soc. 98 (1976) 1287.
[13] J.A. Kirby, D.B. Goodin, T. Wydrzynski, A.S. Robertson, M.P. Klein, J. Am. Chem. Soc. 103 (1981) 5537.
[14] S.D. Conradson, D.L. Clark, M. P Neu, W. Runde, C.D. Tait, Los Alamos Science 26 (2000) 418.
[15] S.C.B. Myneni, Sci. Mag. 295 (2002) 1039.
[16] V.I. Nefedov, V.G. Yarzhemsky, A.V. Chuvaev, E.M. Trishkina, J. Electron Spectrosc. Relat. Phenom. 46 (1988) 381.
[17] F.E. Huggins, G. Huffman, Fuel 74 (1995) 556.
[18] A. Filipponi, T.A. Tyson, K.O. Hodgson, S. Mobilio, Phys. Rev. A 48 (1993) 1328.
[19] E.M. Moujahid, J.P. Besse, F. Leroux, J. Mater. Chem. 13 (2003) 258.
[20] R.J. Kirkpatrick, P. Yu, X. Hou, Y. Kim, Am. Mineral. 84 (1999) 1867.